(Pro)renin receptor-mediated myocardial injury, apoptosis, and inflammatory response in rats with diabetic cardiomyopathy

Received for publication, January 21, 2019, and in revised form, March 29, 2019 Published, Papers in Press, April 5, 2019, DOI 10.1074/jbc.RA119.007648

Xuefei Dong[‡§1], **Shiran Yu**[‡¶1], **Ying Wang**[‡¶¶1], **Min Yang**[‡‖], **Jie Xiong**[‡], **Naier Hei**[‡], **Bo Dong**[‡¶2], **Qing Su**[**3], and **Jing Chen**[‡‡ §§4]

From the [‡]Department of Cardiology, Shandong Provincial Hospital Affiliated to Shandong University, Jinan 250012, China, the [¶]Key Laboratory of Cardiovascular Remodeling and Function Research, Qilu Hospital, Shandong University, Jinan 250012, China, the [§]University of Hull, Hull HU6 7RX, United Kingdom, the [‖]Department of Laboratory, The Third Hospital of Jinan, Jinan 250132, China, the [**]Department of Endocrinology, Shanghai Jiaotong University School of Medicine, Xinhua Hospital, Shanghai 200092, China, the [‡‡]Warwick Medical School, University of Warwick, Coventry CV4 7AL, United Kingdom, the [§§]Jining Medical University, Jining 272113, China, and the [¶¶]Dezhou Municipal Hospital, Dezhou City, Shandong Province, Dezhou 253012, China

Edited by Jeffrey E. Pessin

Excessive activation of the renin-angiotensin system (RAS) in diabetic cardiomyopathy (DCM) provokes a series of structural and functional abnormalities, and causes ventricular remodeling and heart failure in diabetes. (Pro)renin receptor (PRR) is a component of the RAS and has been reported to be up-regulated in some cardiovascular diseases. Furthermore, PRR blockade in some cardiovascular diseases, such as myocardial infarction and hypertension, has been demonstrated to reverse their pathogenesis. However, there have been few studies about the function of PRR in the pathogenesis of DCM. In this study, we hypothesized that PRR is involved in the pathogenesis of DCM and mediates myocardial injury in DCM. To explore the role of PRR in DCM, we evaluated the effects of PRR overexpression and knockdown on the DCM phenotype *in vivo* and *in vitro*. The results show that PRR overexpression exacerbates myocardial injury and the inflammatory response in rats with DCM. Conversely, PRR knockdown alleviates myocardial fibrosis, apoptosis, and the inflammatory response, reversing the cardiac dysfunction in rats with DCM. In cell experiments, PRR overexpression also up-regulated the protein expression of collagen I and fibronectin, aggravated the inflammatory response, and increased the production of reactive oxygen species, whereas PRR knockdown had the opposite effect. Thus, PRR mediates myocardial injury, apoptosis, and the inflammatory response, likely through a PRR/extracellular signal-regulated kinase/reactive oxygen species pathway.

Diabetes is an important chronic metabolic disease that substantially affects health and lifespan. Diabetic cardiovascular complications are major causes of death in diabetes. Previous studies have shown that diabetes not only exacerbates cardiovascular diseases, including atherosclerosis and hypertension, but is itself responsible for cardiac injury (1). Diabetic cardiomyopathy is one of the most serious complications of diabetes and is characterized by a series of structural and functional abnormalities, including myocardial fibrosis, inflammation, cellular apoptosis, and ventricular remodeling (2). A previous study showed that treatment aimed at alleviating myocardial fibrosis, apoptosis, and inflammation is protective against cardiac pathology in diabetic cardiomyopathy (DCM)[5] (3).

Excessive activation of the renin-angiotensin system (RAS) is reported to be important in the pathogenesis of DCM. RAS activation can induce or exacerbate myocardial fibrosis, oxidative stress, inflammation, and other pathological changes. However, although angiotensin-converting enzyme inhibitors and angiotensin receptor blockers are widely used in clinical practice, they do not substantially reduce the morbidity and mortality associated with the cardiovascular complications of diabetes. Thus, it is necessary to identify potential new therapeutic targets, the use of which might be associated with more satisfactory outcomes (4, 5).

(Pro)renin receptor (PRR) is a member of the RAS that was recently discovered and is widely expressed in blood vessels, the heart, and kidneys. PRR is a single transmembrane protein that binds both renin and prorenin, and has been implicated in a number of cardiovascular diseases (6, 7). Binding of ligand to PRR leads to renin activation and nonproteolytic activation of

This work was supported by National Natural Science Foundation of China Grants 81870283, 81570729, and 81170207 and Program of State Chinese Medicine Administration Bureau Grant JDZX2012113. The authors declare that they have no conflicts of interest with the contents of this article.

[1] These authors contributed equally to the results of this work.

[2] To whom correspondence may be addressed: Shandong Provincial Hospital affiliated to Shandong University. No. 324, Jing 5 Road, Jinan, Shandong 250012, China. Tel.: 86-531-68777840; Fax: 86-531-68777840; E-mail: bodong@sdu.edu.cn.

[3] To whom correspondence may be addressed: Dept. of Endocrinology, Xinhua Hospital, Shanghai Jiaotong University School of Medicine, 1665 Kongjiang Rd., Shanghai 200092, China. Tel.: 86-21-25077530; Fax: 86-21-25077532; E-mail: suqing@xinhuamed.com.cn.

[4] To whom correspondence may be addressed: Warwick Medical School, University of Warwick, Coventry CV4 7AL, United Kingdom. Tel.: 44-0-2476574880; Fax: 44-0-2476574880; E-mail: Jing.Chen@warwick.ac.uk.

[5] The abbreviations used are: DCM, diabetic cardiomyopathy; RAS, renin-angiotensin system; PRR, (Pro)renin receptor; AngII, angiotensin II; MAPK, mitogen-activated protein kinase; shRNA, short hairpin RNA; eGFP, enhanced green fluorescent protein; IL, interleukin; SOD, superoxide dismutase; MDA, malondialdehyde; LVEF, left ventricular ejection fraction; LVEDD, left ventricular end-diastolic diameter; LVESD, left ventricular end-systolic diameter; ERK, extracellular signal-regulated kinase; DHE, dihydroethidium; STZ, streptozotocin; GAPDH, glyceraldehyde-3-phosphate dehydrogenase; DMEM, Dulbecco's modified Eagle's medium; FBS, fetal bovine serum.

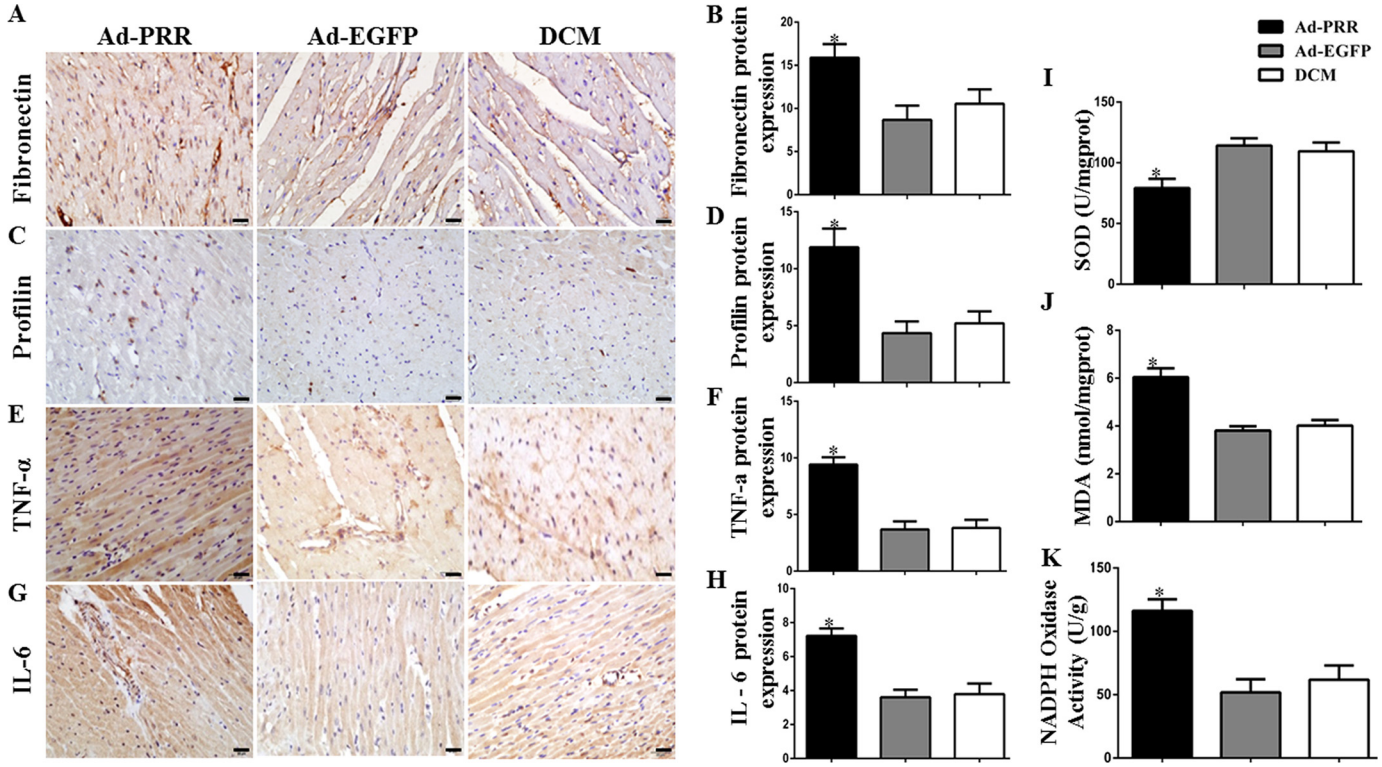

Figure 1. The level of myocardial fibrosis, inflammation response, and oxidative stress response in the Ad-PRR, Ad-EGFP, and DCM groups. *A,* immunostaining of fibronectin; *B,* quantitative analysis of the results shown in *A*. *C,* immunostaining of profilin. *D,* quantitative analysis of the results shown in *C*. *E,* immunostaining of tumor necrosis factor (*TNF*) α. *F,* histograms (*right*) showing the quantitative analysis of the positive staining of *E*. *G,* immunostaining of IL-6. *H,* quantitative analysis of the positive staining of *G*. *I,* SOD contents. *J,* MDA contents. *K,* NADPH oxidase activity in 3 groups; *, $p < 0.05$ compared with the DCM and Ad-EGFP groups. *Scale bar* = 20 μm, magnification ×40.

prorenin, the formation of angiotensin II (AngII), and the activation of a variety of AngII-independent signal transduction pathways, such as the mitogen-activated protein kinase (MAPK) signaling pathway (8). This dual function has led to the identification of PRR as a potentially efficient therapeutic target. Specific PRR inhibition has been demonstrated to be beneficial in a range of diseases, including hypertension and diabetic nephropathy (9, 10). Although few studies have evaluated the effects of PRR blockade in DCM, one recent study found that PRR expression in the myocardium is high in a rat model of DCM (11).

We hypothesized that PRR mediates myocardial injury, apoptosis, and inflammatory responses in DCM. To evaluate the respective effects of PRR overexpression and knockdown on myocardial injury, apoptosis, and inflammatory responses in DCM, we conducted experiments in Wistar rats and cardiac fibroblasts *in vitro*. We overexpressed or silenced PRR expression using adenoviruses (Ad-PRR and Ad-PRR-short hairpin RNA (shRNA), respectively) and established a potential mechanism for the role of PRR in DCM.

Results

The effects of PRR overexpression and knockdown on myocardial injury

First, the effects of PRR overexpression on myocardial injury were determined. Immunohistochemistry revealed that fibronectin protein expression was higher in Ad-PRR–treated rats than in the DCM control group or in the adenoviruses carried enhanced GFP (Ad-EGFP)–treated group (Fig. 1, *A* and *B*, $p < 0.05$). The expression of profilin showed a similar trend, with expression in the Ad-PRR group being significantly higher than that in the DCM and Ad-EGFP groups (Fig. 1, *C* and *D*, $p < 0.05$).

Second, the effects of PRR knockdown on myocardial fibrosis were also evaluated. The protein expression of collagen I and fibronectin in the three groups was also evaluated using immunohistochemistry, showing that collagen I expression was significantly lower in the Ad-PRR-shRNA group than in the DCM or Ad-SC-shRNA group (Fig. 2, *A* and *B*, $p < 0.01$), and a similar trend for the expression of fibronectin (Fig. 2, *C* and *D*, $p < 0.05$).

In addition, the extent of cellular apoptosis was assessed using a terminal deoxynucleotidyl transferase dUTP nick-end labeling (TUNEL) assay, which showed that the percentage of apoptotic cells in the Ad-PRR-shRNA group was much lower than that in the DCM and Ad-SC-shRNA groups (Fig. 2, *E* and *F*, $p < 0.01$).

The effects of PRR overexpression and knockdown on myocardial inflammation

First, tumor necrosis factor-α and interleukin (IL)-6 protein expression was also evaluated using immunohistochemistry after PRR overexpression, showing that both were significantly higher in the Ad-PRR group than in the DCM and Ad-EGFP groups (Fig. 1, *E–H*, $p < 0.05$).

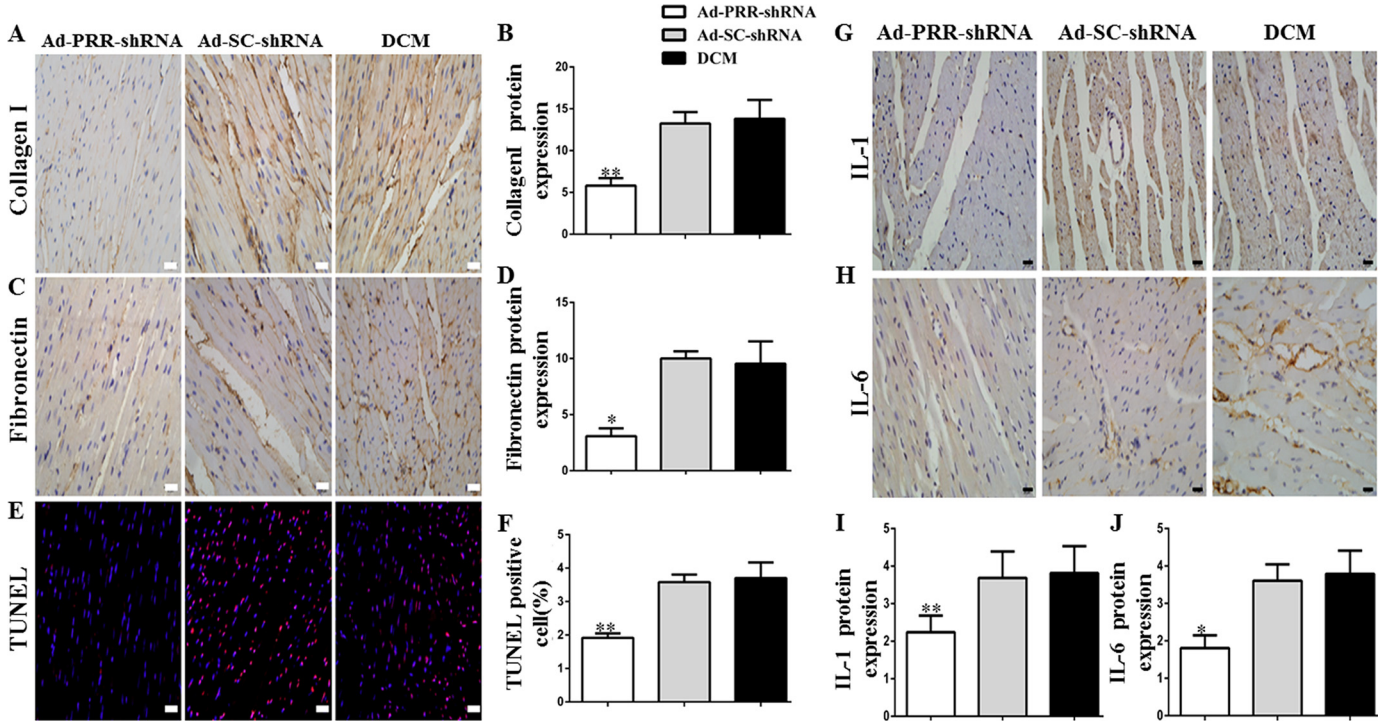

Figure 2. The levels of collagen I, fibronectin, IL-1, IL-6 protein expressions, and TUNEL assay in 3 groups. *A,* immunostaining of collagen I. *B,* quantitative analysis of the results shown in *A*. *C,* immunostaining of fibronectin. *D,* quantitative analysis of the results shown in *C*. *E,* representative images and analysis of the TUNEL assay. *F,* quantitative analysis of the results shown in *E*. *G,* immunostaining of IL-1. *I,* histograms (*right*) showing the quantitative analysis of the positive staining of IL-1. *H,* immunostaining of IL-6. *J,* quantitative analysis of the positive staining of IL-6 in DCM, Ad-SC-shRNA, and Ad-PRR-shRNA groups. *, $p < 0.05$; **, $p < 0.01$ compared with the DCM and Ad-SC-shRNA groups. *Scale bar* = 20 μm, magnification ×40.

Second, after PRR knockdown in DCM, immunohistochemistry revealed that IL-1 protein expression in myocardium was significantly lower in the Ad-PRR-shRNA group than in the DCM and Ad-SC-shRNA groups (Fig. 2*G*, $p < 0.01$). Furthermore, the protein expression of IL-6 showed the same pattern (Fig. 2*H*, $p < 0.05$).

The effects of PRR overexpression and knockdown on superoxide dismutase and NADPH oxidase activities and malondialdehyde content

Superoxide dismutase (SOD) activity and malondialdehyde (MDA) content were measured after PRR overexpression. SOD activity in the Ad-PRR group was lower than in the DCM and Ad-EGFP groups (Fig. 1*I*, $p < 0.05$), whereas the MDA content in the Ad-PRR group was higher than in the DCM and Ad-EGFP groups (Fig. 1*J*, $p < 0.05$). In addition, NADPH oxidase activity was higher in the Ad-PRR group than in the DCM and Ad-EGFP groups (Fig. 1*K*, $p < 0.05$).

After PRR knockdown, SOD content in the Ad-PRR-shRNA group was higher than in the DCM and Ad-SC-shRNA groups (Fig. 3*A*, $p < 0.05$). By contrast, compared with the DCM and Ad-SC-shRNA groups, the MDA content in the Ad-PRR-shRNA group was lower (Fig. 3*B*, $p < 0.05$). Furthermore, NADPH oxidase activity was significantly lower in the Ad-PRR-shRNA group than in the DCM and Ad-SC-shRNA groups (Fig. 3*C*, $p < 0.01$).

Effect of PRR silencing on cardiac function

At the end of the study period, cardiac function was assessed in the Ad-PRR-shRNA, Ad-SC-shRNA, and DCM groups using echocardiography. This showed that the left ventricular ejection fraction (LVEF) was higher in the Ad-PRR-shRNA group than in the DCM and Ad-SC-shRNA groups (Fig. 3*D*, $p < 0.05$). Both the left ventricular end-diastolic diameter (LVEDD) and the left ventricular end-systolic diameter (LVESD) were lower in the Ad-PRR-shRNA group than in the DCM and Ad-SC-shRNA groups (Fig. 3*E*–F, $p < 0.05$). With regard to diastolic function, the ratio of flow Doppler E wave to A wave amplitude (E/A ratio) was much higher in the Ad-PRR-shRNA group than in the DCM and Ad-SC-shRNA groups (Fig. 3*G*, $p < 0.01$).

Effects of PRR overexpression or silencing on ROS production and activation of the extracellular signal-regulated kinase pathway in vitro

In the first instance, the degree of PRR protein overexpression in the cardiac fibroblasts was determined using Western blotting, which showed that PRR protein expression was significantly higher in Ad-PRR-treated cells than in Ad-EGFP-treated or high glucose-treated cells (Fig. 4, *A* and *B*, $p < 0.01$). However, the addition of the extracellular signal-regulated kinase (ERK) inhibitor PD98059 did not affect PRR protein expression.

The effects of PRR overexpression on cardiac fibroblasts were also assessed. Western blotting showed that ERK phosphorylation was lower in Ad-PRR + PD98059-treated cells than in Ad-PRR-infected cells (Fig. 4, *C* and *D*, $p < 0.05$). Dihydroethidium (DHE) assay showed that ROS production was higher in Ad-PRR-infected cells than in high glucose-treated or Ad-EGFP-infected cells, but lower in Ad-PRR + PD98059-treated cells than in Ad-PRR-infected cells (Fig. 4, *E* and *F*, $p < 0.05$).

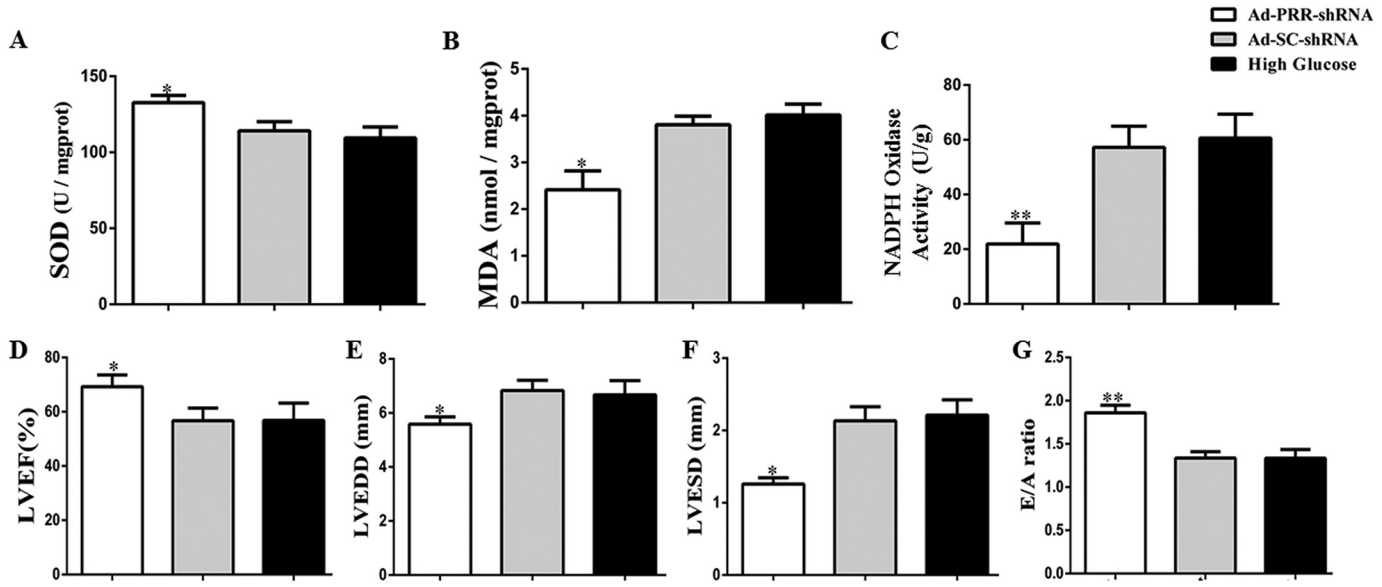

Figure 3. Oxidative stress response levels and cardiac function data in 3 groups of rats. *A*, SOD contents; *B*, MDA contents; *C*, NADPH oxidase activity; *D*, indicated LVEF; *E*, LVEDD; *F*, LVESD; and *G*, ratio of peak early to late diastolic filling velocity (E/A ratio) respective to levels in the 3 groups in DCM, Ad-SC-shRNA, and Ad-PRR-shRNA groups.

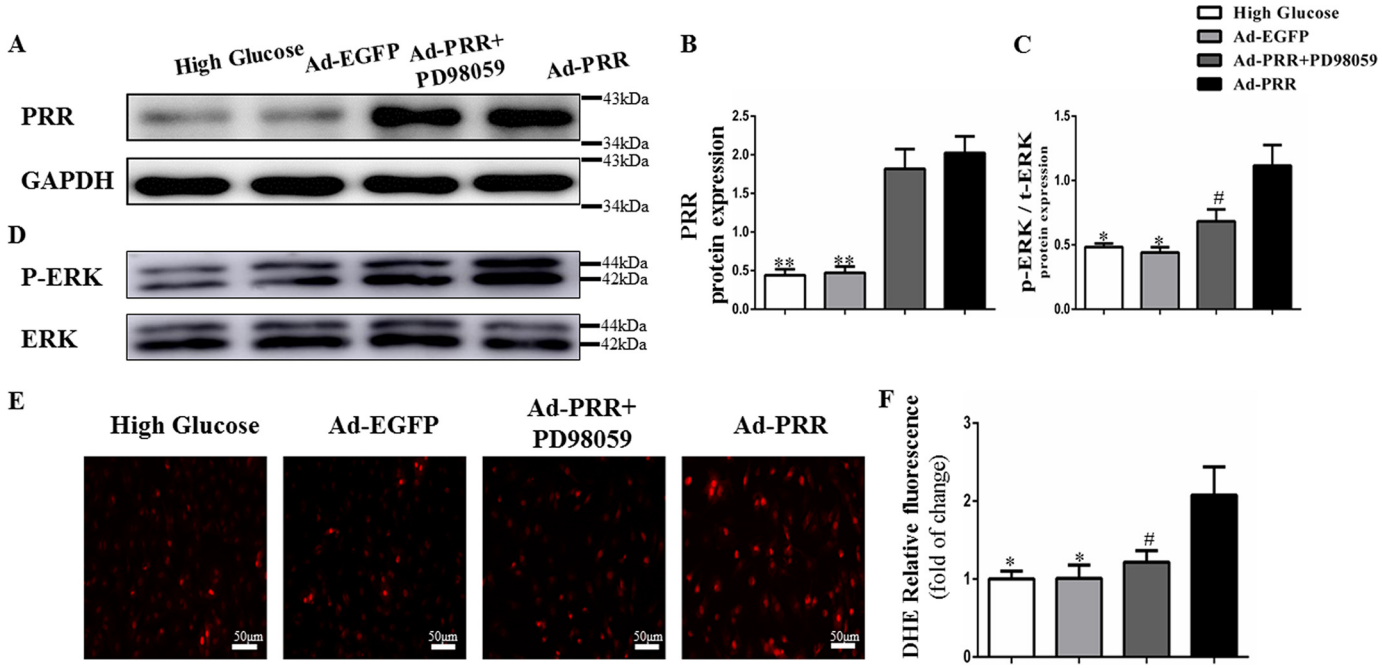

Figure 4. PRR protein, *p*-ERK, *t*-ERK protein expression, and oxidative stress response level in cardiac fibroblasts in high glucose, Ad-EGFP, Ad-PRR, and Ad-PRR + PD98059 groups. *A*, Western blotting showing PRR protein expression. *B*, quantitative analysis of the results shown in *A*. *D*, Western blotting showing *p*-ERK, *t*-ERK protein expression. *C*, quantitative analysis of the results shown in *D*. *E*, DHE showing ROS production in 3 groups. *F*, quantitative analysis of the results shown in *E*. *, $p < 0.05$; **, $p < 0.01$ compared with the high glucose and Ad-EGFP groups; #, $p < 0.05$ compared with Ad-PRR group. *Scale bar* = 50 μm, magnification ×20.

We next measured PRR protein expression in Ad-PRR-shRNA–infected cells, and found that it was much lower than in high glucose–treated or Ad-SC-shRNA–infected cells (Fig. 6, *A* and *B*, $p < 0.05$). In these cardiac fibroblasts, Western blotting showed that ERK phosphorylation was lower in Ad-PRR-shRNA–infected cells than in high glucose–treated or Ad-SC-shRNA–infected cells (Fig. 6, *C* and *D*, $p < 0.05$). DHE assay showed that ROS production was lower in Ad-PRR-shRNA–infected cells than in high glucose–treated or Ad-SC-shRNA–infected cells (Fig. 6, *E* and *F*, $p < 0.05$).

The effects of PRR overexpression and silencing on collagen I, fibronectin, IL-1, and IL-6 protein expression in vitro

Collagen I and fibronectin gene and protein expression was measured using PCR and ELISA, respectively, in the cardiac fibroblasts. This showed that the expression of both genes at the mRNA and protein levels was higher in Ad-PRR–infected cells than in high glucose–treated or Ad-EGFP–infected cells, but lower in Ad-PRR + PD98059 –treated cells (Fig. 5, *A–D*, $p < 0.05$). IL-1 and IL-6 expression was also measured using PCR and ELISA, which showed that both were expressed at lower

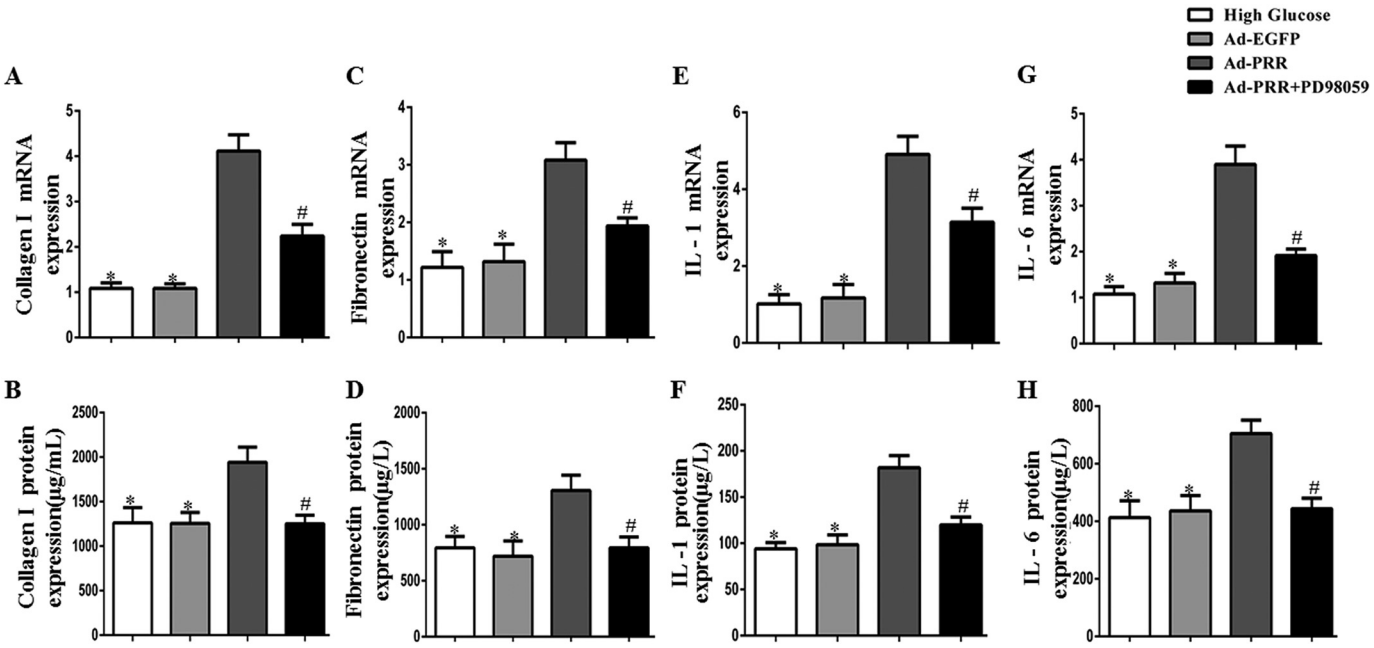

Figure 5. Collagen I, fibronectin, IL-1, IL-6 expression in the high glucose, Ad-EGFP, Ad-PRR, and Ad-PRR + PD98059 groups *in vitro* in cardiac fibroblasts. *A,* collagen I mRNA expression; *B,* ELISA of collagen I protein expression; *C,* fibronectin mRNA expression; *D,* ELISA of fibronectin protein expression; *E,* IL-1 mRNA expression; *F,* ELISA of IL-1 protein expression; *G,* IL-6 mRNA expression; *H,* ELISA of IL-6 protein expression. *, $p < 0.05$ compared with the high glucose and Ad-EGFP groups; #, $p < 0.05$ compared with Ad-PRR group.

levels in Ad-PRR + PD98059 –treated cells than in Ad-PRR–infected cells at both the mRNA and protein levels (Fig. 5, *E–H*, $p < 0.05$).

Next, the effects of PRR knockdown on the protein expression of collagen I and fibronectin were measured. The ELISA results showed that the protein expression of collagen I and fibronectin was lower in Ad-PRR-shRNA–infected cells than in high glucose–treated or Ad-SC-shRNA–infected cells (Fig. 6, *G* and *H*, $p < 0.05$). The same pattern of protein expression was also identified for IL-1 and IL-6 using ELISA (Fig. 6, *I* and *J*, $p < 0.05$).

Discussion

In this study, we have shown that PRR overexpression exacerbates myocardial injury, increases the inflammatory response, and increases oxidative stress in an animal model of DCM. By contrast, knockdown of PRR protein expression using RNAi ameliorates fibrosis, the inflammatory response, apoptosis, and defects in cardiac function in rats with DCM. In cardiac fibroblasts *in vitro*, we showed that PRR overexpression increases the production of ROS, activates the ERK pathway, and further increases the expression of collagen I, fibronectin, IL-1, and IL-6, at both the mRNA and protein levels. However, treatment with the ERK inhibitor PD98059 ameliorates the adverse gene expression profile resulting from PRR overexpression. In addition, PRR knockdown prevented the effects of high glucose–induced PRR up-regulation. Taken together, our findings indicate that PRR mediates myocardial injury, apoptosis, and the inflammatory response in DCM via a PRR/ERK/ROS pathway.

DCM is one of most serious cardiovascular complications of diabetes. It is characterized by several myocardial structural and functional abnormalities (1). The key components of the pathogenesis of DCM are myocardial fibrosis, left ventricular remodeling, and cardiac dysfunction (2). An important pathological feature of DCM is the accumulation of extracellular matrix proteins, and a previous study demonstrated that the accumulation of extracellular matrix is induced by hyperglycemia (12). Singh *et al.* found that both intracellular and extracellular AngII contribute to the greater fibrosis mediated by cardiac fibroblasts in a high glucose environment (12). Related studies have found that the binding of renin or prorenin to PRR leads to renin activation and nonproteolytic activation of prorenin, which induced further AngII synthesis and the activation of a variety of AngII-independent signal transduction pathways, which promote myocardial fibrosis. A recent clinical study showed that serum-soluble (pro)renin receptor concentrations reflects the severity of heart failure (13). Thus, lower PRR expression in disease models could reverse the pathogenesis of such diseases (14). The multiple functionality of PRR has led to it being thought of as a potentially novel and efficient therapeutic target for certain cardiac diseases. The present study has shown that PRR knockdown improves cardiac function, assessed using echocardiography in rats with DCM, which suggests that PRR down-regulation might be able to ameliorate the cardiac dysfunction associated with DCM.

Previous studies show that metabolic disturbances associated with DCM often result in fibrosis and inflammation, and that these lead directly to contractile dysfunction (15). Ellmers *et al.* (16) demonstrated that inhibition of PRR after myocardial infarction in mice ameliorates the cardiac fibrosis and impairment in cardiac dysfunction. Furthermore, inhibition of PRR attenuates mesangial cell proliferation and reduces the associated renal fibrosis (17). The present study has shown that PRR overexpression is associated with higher protein expression of

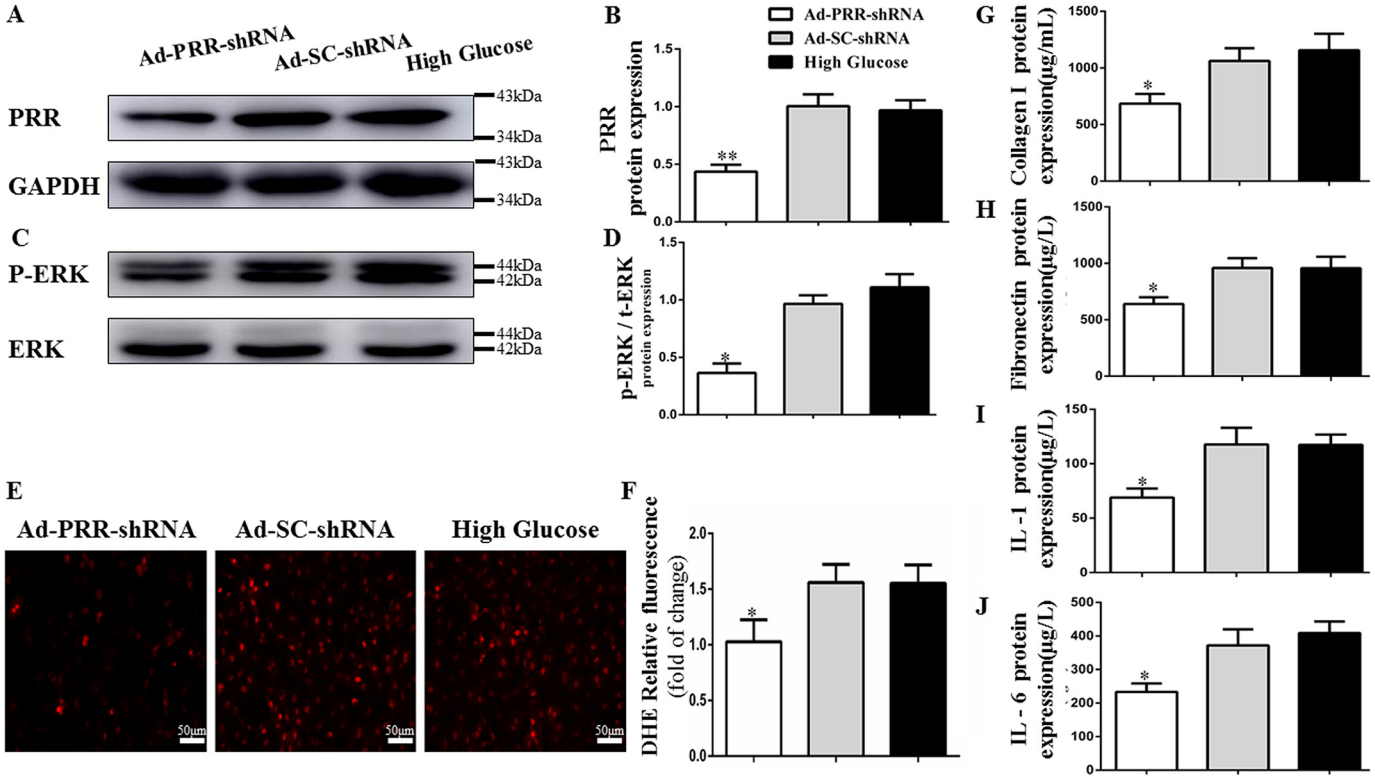

Figure 6. PRR protein, *p*-ERK, *t*-ERK protein expression; fibrosis, inflammation, and oxidative stress response level in 3 groups' cardiac fibroblasts. *A,* Western blotting showing PRR protein expression. *B,* quantitative analysis of the results shown in *A*. *C,* Western blotting showing *p*-ERK, *t*-ERK protein expression. *D,* quantitative analysis of the results shown in *C*. *E,* DHE showing ROS production in 3 groups. *F,* quantitative analysis of the results shown in *E*. *G–J,* ELISA of collagen I, fibronectin, IL-1, and IL-6 protein expression in the high glucose, Ad-SC-shRNA, and Ad-PRR-shRNA groups. *, $p < 0.05$; **, $p < 0.01$ compared with the high glucose and Ad-SC-shRNA groups. *Scale bar* = 50 μm, magnification ×20.

fibronectin and profilin, whereas knockdown of PRR expression using RNAi reduces the expression of collagen I and fibronectin in DCM rats. Collectively, this implies that PRR is involved in myocardial fibrosis in DCM. In addition, PRR knockdown inhibits cellular apoptosis in DCM. In addition, PRR overexpression and knockdown had complementary effects in high glucose–treated cardiac fibroblasts *in vitro*. Thus, the findings of the present and previous studies show that PRR is involved in determining the extent of myocardial injury in DCM.

With regard to the inflammatory response, Kanda and Ishida (18) recently reported that PRR RNAi in rats alleviates the inflammation associated with diabetic retinopathy. The *in vivo* and *in vitro* findings of the present study are consistent with this, because PRR overexpression was found to aggravate the inflammatory response in DCM and to exacerbate the high glucose–induced inflammatory response in cardiac fibroblasts, whereas PRR silencing had the opposing effect, ameliorating some of the deleterious changes associated with DCM. Thus, PRR also seems to play a role in the regulation of the inflammatory response in DCM.

The recent study by Rani *et al.* (19) showed that during hyperglycemia there are changes to the redox status of cardiac cells, such that antioxidant therapy may be protective against the effects of hyperglycemia. In addition, antioxidant therapy has been shown to alleviate inflammation and fibrosis, and thus to ameliorate the pathogenesis of cardiac complications in diabetic rats (20). Taken together, these findings imply that the exploitation of an antioxidant mechanism may be a viable therapeutic approach for DCM. In the present study, we found that PRR overexpression in DCM exacerbates oxidative stress, whereas PRR knockdown reduces oxidative stress in DCM rats. Our *in vitro* data also demonstrate that high glucose–induced ROS production is further up-regulated after PRR overexpression, whereas PRR knockdown has the opposite effect. Thus, the regulation of myocardial injury and the inflammatory response by PRR in DCM appear to be mediated through its antioxidant effects.

It has been reported that PRR activation in mouse renal collecting duct cells increases fibrosis via MAPK-dependent ROS accumulation (21). We showed here that PRR overexpression increases ERK phosphorylation in a high glucose environment, whereas PRR knockdown significantly ameliorates this effect. We then showed that the ERK inhibitor PD98059 prevents the PRR overexpression–induced activation of the ERK pathway, reducing ROS production, and inhibiting the changes involved in myocardial fibrosis and the inflammatory response in DCM. Thus, the effect of PRR on myocardial injury, the inflammatory response, and apoptosis is mainly associated with activation of the PRR/ERK/ROS pathway in DCM.

In conclusion, PRR is an important component of the RAS and can regulate myocardial injury, the inflammatory response, and apoptosis in DCM. The underlying mechanism involves greater ROS production mediated through the ERK pathway. This implies that inhibition of PRR could represent a novel therapeutic approach for DCM, and that a beneficial effect

would be dependent on inhibition of the PRR/ERK/ROS pathway.

Experimental procedures

PRR-expressing adenovirus construction

The amplified open reading frame (ORF) of the *PRR* gene, which was designed by the GenePharma Company (Shanghai, China), was inserted into the pDC316 plasmid vector to construct pDC316-*PRR*. Then, the pDC316-*PRR* plasmid or pDC316-*EGFP*, as a control, and adenovirus vector were co-transformed into *Escherichia coli* to create recombinant adenoviruses expressing PRR (Ad-PRR) or EGFP (Ad-EGFP).

PRR shRNA-expressing adenovirus construction

Ad-PRR-shRNA was designed and constructed by the GenePharma Company to achieve PRR RNAi both *in vivo* and *in vitro*. The most efficient Ad-PRR-shRNA of three sequences was selected using Western blot analysis (Ad-PRR-shRNA-547). The target sequence on the PRR gene was GCT CCG TAA TCG CCT GTT TCA. Adenovirus expressing scrambled shRNA (Ad-SC-shRNA) was also constructed as a control.

Experimental animals

Male Wistar rats (6–8 weeks, 200–250 g) were obtained from Shandong University Animal Centre and maintained in an animal room with controlled temperature (22 °C ± 2 °C) and humidity (55% ± 5%), under a 12-h light/dark cycle. The DCM model was established by a single intraperitoneal injection of streptozotocin (STZ) (65 mg/kg), and successful induction was accepted when blood glucose concentration was >11.1 mmol/liters and there were compatible clinical signs.

Rats were subjected to either PRR silencing or PRR overexpression. For the silencing experiment, the rats were randomly divided into four groups ($n = 15$ per group): a control group, a DCM group, an Ad-SC-shRNA group, and an Ad-PRR-shRNA group. Twelve weeks after STZ administration, rats in the Ad-SC-shRNA, Ad-PRR-shRNA, and DCM groups were given an intravenous injection of recombinant adenovirus expressing SC-shRNA (1×10^9 pfu), PRR-shRNA (1×10^9 pfu), or PBS, respectively, via a tail vein. All the rats were maintained on a normal diet after the intravenous injection. Then, 2 weeks after the adenovirus injection, five rats per group were randomly selected to determine the degree of PRR silencing achieved, and the rest were maintained for a further 2 weeks, before further analyses were undertaken.

For the PRR overexpression experiment, the rats were allocated to a DCM group, an Ad-PRR group, or an Ad-EGFP group. Twelve weeks after STZ administration, the rats in the DCM, Ad-PRR, and Ad-EGFP groups were given an intramyocardial injection of 1×10^9 pfu of Ad-PRR (in 200 μl of PBS), Ad-EGFP (in 200 μl of PBS), or PBS only, respectively, in five separate locations of the left ventricular free wall, under anesthesia (10% chloral hydrate, 300 mg/kg) and while being mechanically ventilated with a VIP Bird ventilator (tidal volume, 3.0 ml and respiratory rate, 60 cycles/min; Bird Products Corp., Palm Springs, CA). Two weeks after the Ad-PRR injection, four rats were randomly selected from each group for assessment of the efficiency of PRR overexpression, whereas the remaining animals were maintained for a further 2 weeks, before analyses were undertaken. During the study, one rat in the DCM group, one in the Ad-PRR-shRNA group, and two in the Ad-PRR group died.

The animal procedures undertaken complied with the Guide for the Care and Use of Laboratory Animals from the National Academy of Sciences, published by the United State National Institutes of Health (NIH Publication No. 86-23, revised 1996), and with the Principles of Laboratory Animal Care formulated by the National Society for Medical Research. The study was approved by the Institutional Animal Care and Use Committee of Shandong University (Jinan, Shandong Province, China).

Echocardiography measurements

At the end of each animal study, the rats were anesthetized with 10% chloral hydrate (300 mg/kg, i.p.) for echocardiography using a Vevo770 imaging system (Visual Sonics, Toronto, Canada). M-mode signals, LVEF, the E/A ratio, LVEDD, and LVESD were measured. The values used represented the mean of five consecutive cardiac cycles.

Immunohistochemistry

Immunohistochemical staining was performed using the following steps. The paraffin sections were dewaxed and hydrated, then antigen retrieval was performed at >95 °C using sodium citrate buffer, and nonspecific reactions were blocked with goat serum for 15 min at 37 °C. Then, the sections were incubated with primary polyclonal anti-PRR, anti-collagen I, anti-fibronectin, anti-profilin, anti-IL-1, or anti-IL-6 antibodies (Abcam, Cambridge, MA) overnight at 4 °C, all of which were diluted in 1× PBS to 1:200. Afterward, the sections were incubated with a horseradish peroxidase-labeled secondary antibody (Abcam, Cambridge, MA) for 20–30 min at 37 °C. Negative control sections underwent the same treatment, but without addition of the primary antibody. The sections were then examined under a confocal FV 1000 SPD laser scanning microscope (Olympus Corporation, Tokyo, Japan).

TUNEL assay

Apoptotic cells in the hearts were detected using a TUNEL Assay Kit (*In situ* Direct DNA Fragmentation, Abcam, Cambridge, MA). Images of the processed tissues were captured using fluorescence microscopy with excitation/emission wavelengths of 488/520 nm (Olympus, Japan).

Western blot analysis

Myocardial tissue and cell lysates were prepared, and the proteins were separated by SDS-PAGE and then transferred onto polyvinylidene difluoride membranes. Nonspecific binding was minimized by incubation with 5% skim milk, then the membranes were incubated overnight at 4 °C with specific antibodies diluted 1:1000. The specific primary antibodies used were anti-*p*-ERK, anti-*t*-ERK (Cell Signaling Technology, Danvers MA), anti-(pro)renin receptor (Abcam), and GAPDH (Abcam), and horseradish peroxidase-conjugated secondary antibodies (Abcam) were used to detect specific antigen-anti-

body complex by ChemiDoc Touch Imaging System (Bio-Rad). Densitometry was performed using ImageJ.

Malondialdehyde assay

The MDA content of the myocardium was measured using a commercially available kit based on thiobarbituric acid reactivity (NanJing JianCheng Bioengineering Institute, China). Briefly, after fully mixing 0.1 ml of myocardial tissue homogenate with the reaction reagent, the mixture was heated at 95 °C for 40 min and centrifuged at room temperature, and the supernatant was obtained and mixed with thiobarbituric acid. The T-MDA activity was measured at 532 nm using a spectrophotometer (Thermo Fisher Scientific, USA) and is expressed as units/mg of protein.

Superoxide dismutase assay

Myocardial tissue homogenate was also used to measure SOD activity by a superoxide dismutase (SOD) assay kit (NanJing JianCheng Bioengineering Institute, China). When reacting with the chromogenic reagent, a purple color was produced at an intensity proportional to the nitrate content of the solution. The absorbance of each sample was quantified at 550 nm using the spectrophotometer, and T-SOD activity was expressed as units/mg of protein.

NADPH oxidase activity

NADPH oxidase activity was measured in myocardial tissue homogenates using a NADPH oxidase assay kit (Nan Jing Jian Cheng Bioengineering Institute, China). The absorption of the mixture was measured at 600 nm for 20 and 80 s after the end of the reaction.

Cell culture and treatments

Cardiac fibroblasts were obtained from the myocardium of 1–3– day-old rats. Whole heart was extracted and cut into the smallest pieces possible, then the myocardial matrix was digested using collagenase. The cell suspension was then cultivated for 1.5 h to distinguish cardiac fibroblasts from myocardial cells, according to their different growth rates. The supernatant was then discarded, and the myocardial fibroblast culture medium was added. The cells were cultured in a humidified atmosphere of 5% CO_2 and 95% air at 37 °C until a typical growth pattern was observed. The culture medium consisted of endotoxin-free Dulbecco's modified Eagle's medium (DMEM; Thermo Fisher Scientific, USA) supplemented with 5.6 mM glucose and 10% fetal bovine serum (FBS; Thermo Fisher Scientific, USA). The cardiac fibroblasts were identified by the detection of vimentin expression, and second- to third-generation cardiac fibroblasts were transplanted into six-well plates for further experiments. The fibroblasts were used for either PRR silencing or overexpression. In addition, cells were either maintained in 5.6 mM glucose or switched to 25 mM glucose for 24 h to simulate the effects of hyperglycemia.

Ad-shRNA infection in vitro

Cells were cultivated in DMEM without FBS for more than 12 h, then infected with Ad-SC-shRNA or Ad-PRR-shRNA, or left uninfected. Adenovirus with an assured multiplicity of infection of up to 150:1 was added to each well. After 12 h incubation in transfection reagent, the cells were then switched to normal medium for another 12 h, and then used for further experiments.

Ad-PRR infection and treatment of cardiac fibroblasts in vitro

The cells were cultivated in DMEM without FBS for more than 12 h, then infected with Ad-PRR or Ad-EGFP, or not infected. Adenovirus with an assured multiplicity of infection of up to 150:1 was added to each well. After 12 h incubation in transfection reagent, the cells were then switched to normal medium for another 12 h, and then used for further experiments. Some cells were also pre-treated with the ERK inhibitor PD98059 (15 μM, Selleck, Houston, TX) in normal glucose culture medium for 1 h, and then placed in medium containing 25 mM glucose ± ERK inhibitor (PD98059) for another 12 h.

RNA extraction and real-time PCR

Total RNA was isolated from myocardial tissues and cardiac fibroblasts using TRIzol Reagent (Thermo Fisher Scientific, USA). The purified RNA was diluted in diethylpyrocarbonate-treated water, and the concentration was determined. cDNA was synthesized from 1 mg of total RNA using a Prime Script 1st Strand cDNA Synthesis Kit (Takara, Japan).

Gene expression was analyzed by real-time PCR using a Roche LightCycler 480 sequence detection system. PCR was performed in 20-μl reaction mixtures containing SYBR® Premix Ex Taq™ II using 40 amplification cycles. Each sample was analyzed in triplicate. The primers for rat IL-1, IL-6, collagen I, fibronectin, PRR, and GAPDH were purchased from the Bio-Sune Company, and the cycling parameters used followed the manufacturer's recommendations. The following primer sequences were used: PRR: forward, 5′-TCTGTTCTCAACTCGCTCCC-3′, reverse, 5′-TCTCCATAACGCTTCCCAAG-3′; IL-1β: forward, 5′-GCCACCTTTTGACGTGATGAG-3′, reverse, 5′-AGCTTCTCCACAGCCACAAT-3′; IL-6: forward, 5′-CCCACCAGGAACGAAAGTCAA-3′, reverse, 5′-CTGGAAGTCTCTTGCGGAG-3′; Collagen I: forward, 5′-CACTGCAAGAACAGCGTAGC-3′, reverse, 5′-AAGTTCCGGTGTGACTCGTG-3′; Fibronectin: forward, 5′-ACAGCATCAGTGTCAGGTGG-3′, reverse, 5′-TAGGGCGGTCAATGTTGGTC-3′; GAPDH: forward, 5′-TCTCTGCTCCTCCCTGTTCT-3′, reverse, 5′-ATCCGTTCACACCGACCTTC-3′. GAPDH was used as the reference gene. Relative quantification of the amplified cDNAs was achieved using a LightCycler 480 (Roche, Switzerland), and the target gene expression values were normalized to the expression of GAPDH mRNA.

Measurement of ROS content

ROS content was quantified using the oxidant-sensitive fluorescence probe DHE (Sigma). Cells were washed using serum-free medium three times and then incubated with DHE (5 μM) for 30 min. Afterward, images were captured at excitation/emission wavelengths of 535/610 nm. The fluorescence intensity was quantified using Imagine Plus Pro analysis software (Media Cybernetics Inc., MD) in a blinded fashion.

ELISA

Cell supernatants were collected to determine the concentrations of collagen I, fibronectin, IL-1, and IL-6. All the concentrations were measured using kits, according to the manufacturer's instructions (Abcam). Each experiment was conducted at least in triplicate. The optical density of each sample was determined at 450 nm using an Enzyme Standard Instrument (Thermo Fisher Scientific, USA) and used to calculate the concentration of each protein in the medium.

Statistical analysis

Statistical analyses were performed using SPSS 19.0 software (IBM, Armonk, NY). All data are expressed as the mean ± S.D. of at least three independent experiments. The differences were analyzed using one-way analysis of variance. After one-way analysis of variance analysis, and least significant difference were used to assess the statistical significance of the observed differences between groups. A statistically significant difference was considered to be present at $p < 0.05$.

Author contributions—X. D., Y. W., M. Y., J. X., and N. H. resources; X. D., S. Y., Y. W., M. Y., J. X., and N. H. investigation; X. D., S. Y., Y. W., M. Y., J. X., and N. H. methodology; X. D., S. Y., and Y. W. writing-original draft; X. D., S. Y., and Y. W. project administration; S. Y., J. X., and B. D. writing-review and editing; M. Y., B. D., Q. S., and J. C. formal analysis; B. D., Q. S., and J. C. conceptualization; B. D., Q. S., and J. C. data curation; B. D., Q. S., and J. C. supervision.

References

1. Mizamtsidi, M., Paschou, S. A., Grapsa, J., and Vryonidou, A. (2016) Diabetic cardiomyopathy: a clinical entity or a cluster of molecular heart changes? *Eur. J. Clin. Investig.* **46,** 947–953 CrossRef Medline
2. Jia, G., Hill, M. A., and Sowers, J. R. (2018) Diabetic cardiomyopathy: an update of mechanisms contributing to this clinical entity. *Circ. Res.* **122,** 624–638 CrossRef Medline
3. Zhang, L., Ding, W. Y., Wang, Z. H., Tang, M. X., Wang, F., Li, Y., Zhong, M., Zhang, Y., and Zhang, W. (2016) Early administration of trimetazidine attenuates diabetic cardiomyopathy in rats by alleviating fibrosis, reducing apoptosis and enhancing autophagy. *J. Transl. Med.* **14,** 109 CrossRef Medline
4. Sivasankar, D., George, M., and Sriram, D. K. (2018) Novel approaches in the treatment of diabetic cardiomyopathy. *Biomed. Pharmacother.* **106,** 1039–1045 Medline
5. Tian, J., Zhao, Y., Liu, Y., Liu, Y., Chen, K., and Lyu, S. (2017) Roles and mechanisms of herbal medicine for diabetic cardiomyopathy: current status and perspective. *Oxid. Med. Cell. Longev.* 2017, 8214541 Medline
6. Rafiq, K., Mori, H., Masaki, T., and Nishiyama, A. (2013) (Pro)renin receptor and insulin resistance: possible roles of angiotensin II-dependent and -independent pathways. *Mol. Cell. Endocrinol.* **378,** 41–45 CrossRef Medline
7. Ribeiro, A. A., Amorim, R. P., Palomino, Z. J., de Paula Lima, M., Moraes-Silva, I. C., Souza, L. E., Pesquero, J. L., Irigoyen, M. C., and Casarini, D. E. (2018) (Pro)renin receptor expression in myocardial infarction in transgenic mice expressing rat tonin. *Int. J. Biol. Macromol.* **108,** 817–825 CrossRef Medline
8. Huber, M. J., Basu, R., Cecchettini, C., Cuadra, A. E., Chen, Q. H., and Shan, Z. (2015) Activation of the (pro)renin receptor in the paraventricular nucleus increases sympathetic outflow in anesthetized rats. *Am. J. Physiol. Heart Circ. Physiol.* **309,** H880–H887 Medline
9. Xu, Q., Jensen, D. D., Peng, H., and Feng, Y. (2016) The critical role of the central nervous system (pro)renin receptor in regulating systemic blood pressure. *Pharmacol. Ther.* **164,** 126–134 Medline
10. Batenburg, W. W., Verma, A., Wang, Y., Zhu, P., van den Heuvel, M., van Veghel, R., Danser, A. H., and Li, Q. (2014) Combined renin inhibition/(pro)renin receptor blockade in diabetic retinopathy: a study in transgenic (mREN2)27 rats. *PloS One* **9,** e100954 CrossRef Medline
11. Connelly, K. A., Advani, A., Kim, S., Advani, S. L., Zhang, M., White, K. E., Kim, Y. M., Parker, C., Thai, K., Krum, H., Kelly, D. J., and Gilbert, R. E. (2011) The cardiac (pro)renin receptor is primarily expressed in myocyte transverse tubules and is increased in experimental diabetic cardiomyopathy. *J. Hypertens.* **29,** 1175–1184 CrossRef Medline
12. Singh, V. P., Baker, K. M., Kumar, R. (2008) Activation of the intracellular renin-angiotensin system in cardiac fibroblasts by high glucose: role in extracellular matrix production. *Am. J. Physiol. Heart Circ. Physiol.* **294,** H1675–H1684 CrossRef Medline
13. Gong, L., Zhang, S., Li, L., Gao, X., Wang, D., Wu, D., Wang, K., and Liu, Y. (2019) Elevated plasma soluble (pro)renin receptor levels are associated with left ventricular remodeling and renal function in chronic heart failure patients with reduced ejection fraction. *Peptides* **111,** 152–157 CrossRef Medline
14. Danser, A. H. (2015) The role of the (pro)renin receptor in hypertensive disease. *Am. J. Hypertens.* **28,** 1187–1196 CrossRef Medline
15. Palomer, X., Pizarro-Delgado, J., and Vázquez-Carrera, M. (2018) Emerging actors in diabetic cardiomyopathy: heartbreaker biomarkers or therapeutic targets? *Trends Pharmacol. Sci.* **39,** 452–467 CrossRef Medline
16. Ellmers, L. J., Rademaker, M. T., Charles, C. J., Yandle, T. G., and Richards, A. M. (2016) (Pro)renin receptor blockade ameliorates cardiac injury and remodeling and improves function after myocardial infarction. *J. Card. Fail.* **22,** 64–72 CrossRef Medline
17. He, M., Zhang, L., Shao, Y., Wang, X., Huang, Y., Yao, T., and Lu, L. (2009) Inhibition of renin/prorenin receptor attenuated mesangial cell proliferation and reduced associated fibrotic factor release. *Eur. J. Pharmacol.* **606,** 155–161 CrossRef Medline
18. Kanda, A., and Ishida, S. (2019) (Pro)renin receptor: involvement in diabetic retinopathy and development of molecular targeted therapy. *J. Diabetes Investig.* **10,** 6–17 CrossRef Medline
19. Preetha Rani, M. R., Anupama, N., Sreelekshmi, M., and Raghu, K. G. (2018) Chlorogenic acid attenuates glucotoxicity in H9c2 cells via inhibition of glycation and PKCα upregulation and safeguarding innate antioxidant status. *Biomed. Pharmacother.* **100,** 467–477 Medline
20. Zhang, L., An, X. F., Ruan, X., Huang, D. D., Zhou, L., Xue, H., Lu, L. M., and He, M. (2017) Inhibition of (pro)renin receptor contributes to renoprotective effects of angiotensin II type 1 receptor blockade in diabetic nephropathy. *Front. Physiol.* **8,** 758 CrossRef Medline
21. Gonzalez, A. A., Zamora, L., Reyes-Martinez, C., Salinas-Parra, N., Roldan, N., Cuevas, C. A., Figueroa, S., Gonzalez-Vergara, A., and Prieto, M. C. (2017) (Pro)renin receptor activation increases profibrotic markers and fibroblast-like phenotype through MAPK-dependent ROS formation in mouse renal collecting duct cells. *Clin. Exp. Pharmacol. Physiol.* **44,** 1134–1144 CrossRef Medline